Research Square

Preprints are preliminary reports that have not undergone peer review.
They should not be considered conclusive, used to inform clinical practice,
or referenced by the media as validated information.

Relaxing P limitation in a P-limited *Eucalyptus* forest rapidly enhances microbial C-N cycling under elevated CO_2

Manon Rumeau

manon.rumeau@univ-pau.fr

LFCR, Université de Pau et des Pays de l'Adour

Fotis Sgouridis

School of Geographical Sciences, University of Bristol

Catriona A. Macdonald

Hawkesbury Institute for the Environment, Western Sydney University

Paola Pisetta Raupp

Hawkesbury Institute for the Environment, Western Sydney University

Charles Warren

School of Life and Environmental Sciences, University of Sydney

Michaela K. Reay

School of Chemistry, University of Bristol

A. Rob MacKenzie

School of Geography, Earth and Environmental Science, University of Birmingham

Sami Ullah

School of Geography, Earth and Environmental Science, University of Birmingham

Yolima Carrillo

Hawkesbury Institute for the Environment, Western Sydney University

Research Article

Keywords: SOM decomposition, P addition, FACE, N depolymerization, compound-specific amino acids, gross mineralization, nitrate, microbial CUE

Posted Date: March 30th, 2026

DOI: https://doi.org/10.21203/rs.3.rs-9245875/v1

License: This work is licensed under a Creative Commons Attribution 4.0 International License.
Read Full License

Additional Declarations: The authors declare no competing interests.

Abstract

Phosphorus (P) can restrict the capacity of forests to store additional carbon (C) with increasing carbon dioxide (CO_2) concentration. Although P limitation is widespread, P addition experiments in mature forests are rare, leaving large uncertainties about whether alleviating P limitation under elevated CO_2 (eCO_2) will enhance C storage or instead shift limitation toward nitrogen (N). Here, we used a parallel P-fertilization x eCO_2 manipulation in a mature forest to investigate the acute nutrient cycling response to P fertilization under eCO_2 with a particular focus on N cycling. In April 2023, a mature P-limited *Eucalyptus* Forest at the Euc-Free Air CO_2 Enrichment (Euc-FACE) experiment in Australia, was fertilized with 1.5 g P m^{-2} following 10 years of CO_2 enrichment. We measured soil gross N mineralization and compound-specific depolymerization rates – offering novel insights into microbial metabolic pathways – alongside extracellular enzymatic activities, and nutrient pools in the top 10 cm of soil before P addition, 10 days and two months afterwards. We found that P addition decreased extracellular soil enzymatic activities associated with C-N-P-mining (– 50%), increased microbial NH_4^+ retention (immobilization: mineralization ratio; + 23%) and microbial C use efficiency (CUE; + 12%), causing a reduction in plant-available N (– 30%) independently from eCO_2. Under eCO_2, P addition stimulated protein depolymerization and C-P enzyme activities. Compound specific analyses revealed increased microbial biosynthesis with P addition via the assimilation of key amino acids such as alanine, glycine and glutamate. These findings indicate that P limitation constrains microbial C-N cycling under eCO_2 by diverting microbial C investment toward P acquisition rather than growth. While alleviating P limitation can rapidly stimulate microbial cycling and promotes microbial C retention under eCO_2, this response may only be transient, as enhanced microbial growth drives the system towards N limitation.

Highlights

• P fertilization in a P-limited forest increased microbial CUE and microbial N retention

• P addition decreased plant available N by 30%, initiating signs of plant-level N limitation

• Following P addition, eCO enrichment increased protein depolymerization rates

1. Introduction

Increasing atmospheric carbon dioxide (CO_2) concentration due to human activities is projected to enhance photosynthesis, mitigating climate change by storing carbon (C) in forest ecosystems (Friedlingstein et al., 2025; Norby, 2025; Zhu et al., 2016). However, this CO_2 fertilization effect can be limited by soil nutrient availabilities, particularly nitrogen (N) and phosphorus (P; Díaz et al., 1993; Jiang et al., 2024b; Reich et al., 2006; Terrer et al., 2018), depending on nutrient plant-acquisition strategies (Terrer et al., 2016). To date, most studies have focused on N-limited ecosystems, where elevated CO_2 (eCO_2) stimulates microbial N cycling to support higher plant growth (Phillips et al., 2011; Rumeau et al.,

2024). However, less is known on how eCO_2 affects nutrient cycling in P-limited ecosystems, which are widespread across the tropics and the southern hemisphere (Du et al., 2020; Ellsworth et al., 2017; Wang et al., 2010). This is a critical gap in knowledge preventing prediction and management of these ecosystems, as the mechanisms behind N and P availability in soil are highly contrasting and unlikely to respond similarly to environmental shifts.

Long term observations from the first Free-Air CO_2 Enrichment (FACE, EucFACE) of a P-limited forest, namely *Eucalyptus* forest in eastern Australia (Crous et al., 2015; Ellsworth et al., 2017) showed that, unlike is common in N limited systems, enhanced photosynthesis did not translate into higher plant biomass (Jiang et al., 2020). Also in contrast to other forests, while soil N pools increased over the first six months of enrichment (Hasegawa et al., 2016), there were no sustained effects on N mineralization (i.e., the release of NH_4^+ from soil organic matter (SOM; Andresen et al., 2020). Further, despite more C being allocated belowground (Jiang et al., 2020), neither P mineralization (Pihlblad et al., 2023) nor P translocation in leaves increased (Crous et al., 2019). Hence, P limitation seems to constrain the processes of microbial activity and enzyme production that allow microbial nutrient-mining of SOM, which could, in turn, support enhanced plant growth (Jiang et al., 2020). However, the extent of this constraint remains uncertain. Given the widespread occurrence of P-limited forests and the observed constraining effect of P on plant response to eCO_2 (Cunha et al., 2022; Ellsworth et al., 2017), P addition experiments are valuable as they offer insights into whether alleviating P limitation enhances forest productivity and C sequestration. Greenhouse P addition experiments resulted in higher plant growth under eCO_2 (Jakobsen et al., 2016; Piñeiro et al., 2023), but such response is likely to be diminished or offset at the ecosystem level due to other nutrient limitation and/or emerging microbe-plant competition (Terrer et al., 2018). To understand the role of P limitation on the CO_2 fertilisation effect, it is necessary to examine these responses at the ecosystem scale.

Beyond direct impacts on plant growth, P limitation alleviation is likely to impact N cycling and availability for plants, with consequences for plant growth. This is because C, N and P cycles are tightly coupled in soils due to the elemental co-occurrence in organic compounds and the relatively constrained C:N:P stoichiometry in plants and microbes (Cleveland and Liptzin, 2007; Griffiths et al., 2012). Alleviating the P limitation that restricts microbial activity and enzyme production, could stimulate N mining from SOM through protein depolymerization (the breakdown of macromolecular organic N into bioavailable free amino acids; FAA) and N mineralization (Chen et al., 2016; Cheng et al., 2018). While N mineralization, is the most commonly measured process (Schimel and Bennett, 2004), the prior biochemical gateway to N mining is protein depolymerization –– a rarely measured process, despite being the rate limiting step for N release into available forms (Noll et al., 2019). Thus, while adding P may stimulate N release from SOM via several pathways, it may also promote its uptake by microbes and plants This could lead to lower N availability and shift the nutrient limitation from P to N (Mooshammer et al., 2014). If N becomes the *new* limiting nutrient for microbes and plants under P addition, the ecosystem response to eCO_2 may completely change. Determining whether alleviating P limitation stimulates N cycling under eCO_2 in P limited systems will help inform biome specific responses to eCO_2

and enable extrapolation of FACE observations to global forest biomes (Norby, 2025). To address this at the ecosystem scale, we assessed the acute (weeks-to-months) soil microbial N cycling response to P addition in a forest after a decade-long CO_2 enrichment. To do this we employed a novel and multifaced methodology using stable ^{15}N isotopic tracing to comprehensively assess microbial dynamics and strategies.

Our aim was to understand if the soil microbial response to eCO_2 is constrained by P limitation, and how shifting the limiting nutrient might modify this response. We utilised the only eCO_2 and P manipulation of a native, mature forest to date, the *Eucalyptus* FACE experiment in eastern Australia, which was fertilized with P in April 2023, following 11 years of continuous CO_2 enrichment. For a comprehensive evaluation of microbial responses, we carried out a high-resolution assessment of multiple N processes and pools by quantifying gross compound-specific depolymerization, N mineralization and N forms in soils before and after the P addition using a ^{15}N pool dilution approach. To reveal shifts in microbial nutrient limitation and microbial strategies (growth vs nutrient acquisition), we measured extracellular soil enzyme activities involved in C, N and P cycling, microbial biomass C, N, and P and calculated microbial C and nutrient use efficiencies. We hypothesize that: 1) eCO_2 alone has little to no impact on N cycling due to strong P-limitation; 2) P-addition will increase microbial N demand, thereby decreasing N availability independently from eCO_2; and 3) under eCO_2, P addition will enhance N-mining from SOM, releasing extra available N potentially available to plants.

2. Materials and Methods

2.1. Experimental site

The study was performed at the EucFACE facility, located in a mature evergreen *Eucalyptus* Forest within a remnant patch of Cumberland Plain Woodland vegetation in Western Sydney, New South Wales (NSW), Australia (33°61'S, 150°74'E). The vegetation is dominated by *Eucalyptus* trees (*Eucalyptus tereticornis L.*) and the understory is composed of a diverse mix of grasses, graminoids, forbs and shrubs (Hasegawa et al., 2018). Soil is classified as Aeric Podosol with areas of Densic Podosol (Australian soil classification; Ross et al., 2020). Soil texture is a loamy sand up to 50 cm followed by a sandy clay loam to about 300 cm deep. This soil is characterized by low fertility and a low P content (Jiang et al., 2024a). From March to May 2023 when the experimental work was undertaken, the site received 149.1 mm of rain (relatively dry period) – for a mean annual precipitation of 1175 mm that year – and the mean temperature over the same period was 16.5°C (Australian Bureau of Meteorology).

The EucFACE facility is composed of six infrastructure rings of 25 m diameter each. Three are fumigated with a concentration of 150 ppm of CO_2 above the ambient concentration (eCO_2) and three are fumigated with air (aCO_2) across the 28 m vertical profile to the top of the canopy (Fig. S1). CO_2 enrichment started in September 2012 and operates all year long during daylight hours and continued over the course of this study. For a detailed site description, see Ellsworth et al. (2017).

2.2. Phosphorus addition treatment

Early April 3rd 2023, four of the six rings, two ambient CO_2, two elevated CO_2, were fertilized with 1.5 g P m^{-2} of superphosphate fertilizer ($Ca(H_2PO_4)_2$; Fig. S1). This application was part of a broader plan to add a total of 3 g P m^{-2}, in order to double the pool of soil inorganic P; (Jiang et al., 2024a). Only four rings were fertilized as the remaining two had been invaded by liana vines, compromising tree health and subsequently their potential response to fertilization. Fertilization was performed after summer to reduce the risk of P leaching by summer heavy rains. To ensure an even distribution of the fertilizer across the soil surface of the rings, the fertilizer was ground, split in weighed portions, blended with washed river sand, and manually applied to 2 x 2 m squares. In each ring, four 2 x 2 m plots were randomly pre-defined for soil sampling, and in each a section of 1 x 1 m was left unfertilized, receiving only washed sand. In total four areas of 1 x 1 m were left unfertilized per ring and each one featured a square (0.5 x 0.5 m) made of aluminium sheet (~ 5 cm high) that was gently inserted ~ 2 cm into the soil to minimize horizontal fertilizer transfer while minimally disturbing roots (Fig. 1).

2.3. Sampling and handling

Soil was sampled in the four rings that received P-addition (ring 1, 2, 3 and 4) in the 2 x 2 m plots designated for soil sampling. Sampling was done three weeks before addition (March 13th), 10 days after addition (April 13th), and approximatively two months after addition (May 29th) in the four 2 x 2 m plots outside and inside the unfertilized squares (Fig. 1). Prior to addition, four soil cores (5 cm diameter, 10 cm depth) were collected in each of the four plots per ring and bulked together to make up a total of four soil samples per ring. Post P-addition, an additional four soil cores were collected from the unfertilized area delimited by aluminium sheets and bulked together to make up a total of four soil samples from the unfertilized areas per ring (Fig. 1B). Collected soil was placed in a cool box, taken to the laboratory and was directly processed for ^{15}N incubation or stored at 4°C for nutrient analyses. Total and fine root biomass (< 2 mm diameter) was assessed by collecting, washing, drying the roots at 60°C for 48 h and weighing the dry mass, which was expressed per volume of soil cores.

2.4. Soil and microbial nutrient pools

To determine soil nutrient pool contents, we quantified soil ammonium ($N\text{-}NH_4^+$), nitrate ($N\text{-}NO_3^-$), free amino acids (FAA), available P (Bray-P), dissolved organic C (DOC), dissolved organic N (DON) and microbial biomass C, N and P (MBC, MBN and MBP, respectively). All nutrient analyses were performed within a week after field collection. Gravimetric moisture was measured by drying ~ 5 g of soil at 70°C for 48 h.

Soil $N\text{-}NH_4^+$ and $N\text{-}NO_3^-$ were measured by extracting 20 g of soil with 60 mL of 1 M potassium chloride (KCl). The extracts were filtered through a Whatman filter paper no #42 and analysed by continuous flow colorimetry (AQ2 discrete analyser; SEAL Analytical, Inc., Mequon, WI, USA). Soil FAA concentration was determined on the same soil extract using the OPAME fluorescence assay described by Jones (2002)

and adapted to a microplate assay by Darrouzet-Nardi et al. (2013). Fluorescence was read after one-hour incubation on a CLARIOstar plate reader (BMG LABTECH, Germany). Bray-P was measured by extracting 3.5 g of soil with 25 mL of Bray extracting solution (0.03 M NH_4F, 0.025 M HCl). The extracts were filtered and analysed by continuous flow colorimetry (AQ2 discrete analyser; SEAL Analytical, Inc., Mequon, WI, USA). Dissolved organic C and N was measured after extraction with 0.05 M K_2SO_4 (1:3 (*w/v*)) and analysis on a TOC-TN analyser (total organic carbon analyser; Shimadzu Corporation, Japan). C, N and P microbial biomass was measured according to the chloroform extraction method (Brookes et al., 1985). For C and N microbial biomass, 2 subsamples of 10 g each were weighed. One was directly extracted with 0.05 M K_2SO_4 while the other one was chloroform-fumigated for 4 days before extraction. C and N were determined in the filtered extracts using a TOC-TN analyzer (total organic carbon analyser; Shimadzu Corporation, Japan). A similar method was applied for microbial biomass P with the difference that fumigation lasted for one day and extraction was done using Bray-P solution – as we assumed that all P is converted to inorganic P during fumigation (Wu et al., 2000) – and analyzed by colorimetry. MBC, MBN, MBP were calculated as the difference in the C, N and P concentrations between the fumigated and the non-fumigated samples. MBC, MBN and MBP were divided by the respective correction factors: K_{EC} = 0.45, K_{EN} = 0.54 and K_{EP} = 0.40 (Halbritter, 2020).

2.5. Ion-exchange resins

Soil NH_4^+, NO_3^- and PO_4^{3-} availabilities were assessed using ion-exchange resin (IER) bags over a period of more than two years (from December 2021 to May 2023) to obtain integrated measurements of nutrient availability. Resin bags contained ~ 15 g of ion exchange resin beads (Dowex Marathon MR-3 hydrogen and hydroxide form; Sigma Aldrich) enclosed in nylon fabric. The bags were acid-washed before use. In each plot, two resins bags were gently inserted in the soil upper layer (0–5 cm). After an incubation time ranging from few days to few months – depending on the campaigns – resins bags were retrieved and stored at –20°C until extraction. Then, resins bags were washed with DI water and extracted with 100 mL of an extraction solution (2 M NaCl, 0.088 M HCl). Extracts were shaken, filtered and stored at –20°C until analysis by continuous flow colorimetry. Concentration in NH_4^+, NO_3^- and PO_4^{3-} were corrected by the mass of resin beads by bag and by the time of incubation to be expressed in ng per mg of resin beads per day.

2.6. ^{15}N pool dilution assays for N process rates assessment

To evaluate if N-mining and microbial N demand were affected by P addition and eCO_2, gross rates of N mineralization, protein depolymerization, microbial immobilization of NH_4^+ and AA were assessed using ^{15}N pool dilution approaches as described by Hart et al. (1994) and Noll et al. (2019) within one week after sampling.

Gross mineralization. Duplicates of fresh soils (20 g) were labelled with 1 mL of ^{15}N enriched $(NH_4)_2SO_4$ (98 atom % ^{15}N, Sigma-Aldrich) solution targeting an enrichment of 0.7 µg ^{15}N per gram of soil corresponding to ~ 30% of the total soil NH_4^+ pool. ^{15}N solution was added dropwise with a syringe and soil was stirred with a spatula to ensure even distribution. Immediately after labelling and following a 24 h incubation at 25°C in the dark, soil samples were extracted with 1 M KCl. NH_4^+ was diffused into acidified filter disks (Davidson et al., 1991) that was analysed for $^{15}N/^{14}N$ ratio analyses using an EA-IRMS (elemental analyser-IRMS: Elementar Isoprime Precision; Elementar Analysensysteme GmbH, Hanau, Germany).

NH_4^+ immobilization over a 24-hour period was determined by measuring the incorporation of ^{15}N into the microbial biomass. In order to do that, another set of soil sample was labelled with 1 mL of ^{15}N enriched $(NH_4)_2SO_4$ solution. After 24 h incubation, the $^{15}N/^{14}N$ ratio of the microbial biomass was determined using the chloroform method (as above) and 15 mL of the K_2SO_4 extracts were dried, ground and encapsulated in tin capsules and analysed with EA-IRMS (see above).

Bulk gross protein depolymerization. Gross depolymerization and AA immobilization rates were measured by the ^{15}N pool dilution method described by Noll et al. (2019). Briefly, triplicates of fresh soils (5 g) were labelled with a solution of ^{15}N enriched amino acids (20 AA mix, Cambridge Isotopes) targeting an enrichment of 0.42 µg ^{15}N per gram of soil corresponding to ~ 30% of the soil FAA pool. Samples were incubated for 0 h, 45 min and 4 h at 25°C in the dark and extracted with 25 mL of 1 M KCl solution. 50 µL of the soil extract was used to quantify the total FAA concentration and the rest of the sample underwent the NH_4^+ diffusion procedure to remove NH_4^+ from the extract before converting FAA into N_2O (oxidation in nitrite and reduction in nitrous oxide) in an air-tight gas exetainer. Post conversion, 1 mL of gas was taken from the reaction mixture and diluted in 20 mL of helium in order to stop the reaction. The ^{15}N content of the N_2O was then determined using a IRMS coupled with a trace-gas pre-concentrator inlet with autosampler (isoFLOW GHG; Elementar Analysensysteme GmbH, Hanau, Germany).

Rates based on ^{15}N pool dilution approach were calculated using equations developed by Kirkham and Bartholomew (1954) and modified by Wanek et al., (2010) for depolymerization and AA immobilization.

Microbial N use efficiency (NUE) was calculated as the amount of N used for growth (i.e. difference between AA immobilization and gross mineralization rate) over the amino acid uptake rate as described by Mooshammer et al., (2014) (1).

$$NUE = \frac{AA\ uptake - N\ mineralization}{AA\ uptake}$$

1

Microbial NH_4^+ immobilization was calculated as follows (2):

$$NH_4^+ \; immobilization \; \left(\mu \; g \; g^{-1} d^{-1}\right) = \frac{\left(\frac{15N\%excess_F}{100} \; x \; N_F\right)_F \; - \; \left(\frac{15N\%excess_{NF}}{100} \; x \; N_{NF}\right)_{NF}}{0.45 \; x \; t}$$

2

Where $15N\%excess_F$ and $15N\%excess_{NF}$ are the atom percent excess of ^{15}N in the extractable N from fumigated (F) and non-fumigated (NF) samples, respectively, and N_F and N_{NF} are the corresponding pools.

Compound specific depolymerization rates. To add insights to gross depolymerization rates and study dynamics of specific AA, compound specific depolymerization rates were measured solely on soils sampled 10 days after P addition. After incubation with solution of ^{15}N enriched AA, 2 mL aliquots of KCl extracts were transferred to an ultrafiltration spin column (10 kDa) which was centrifuged at 3000 rpm for 5 min and ultra-filtered samples were kept frozen for LC-MS analysis. Before analysis, AA were derivatized to increase their hydrophobicity to improve detection limits and enable separation by reversed-phase LC. Derivatization was performed using the AccQ-Tag Ultra Derivatization Kit (Waters, Massachusetts, USA). Briefly, 10 µL of $U^{13}C^{15}N$ alanine standard (1 µg mL^{-1}) was added to 200 µL aliquots of KCl extract and was dried (Vacufuge, Eppendorf). Dried extracts were re-dissolved in 20 µL of 20 mM HCl and 60 µL of borate buffer before adding 20 µL of derivatization agent (in acetonitrile) and heated for 10 minutes. Because KCl is poorly soluble in acetonitrile, the samples were centrifuged to pellet the salts and the supernatant was transferred to a second vial and analysed on a LC-MS instrument. The LC-MS system comprised a nano-LC system (Ultimate 3000 RSLCnano, Thermo Scientific Dionex, Sunnyvale, USA) interfaced via a CaptiveSpray ion source (20 µm tip) to a mass spectrometer (AmaZon SL, Bruker Daltonics, Bremen, Germany). All specifications of the LC-MS characteristics are specified in (Warren, 2019). Amino acids and their isotopomers were detected by their difference in molar mass. Unlabelled and labelled isotopomers were quantified by integrating the area under the curve of the mass corresponding to their protonated pseudomolecular ions (i.e. $[M + H]^+$ ion and $[M + 1 + H]^+$ for an amino acid that contains one ^{15}N). As most amino acids contain only one atom of N, their ^{15}N isotopomer and naturally occurring ^{13}C isotopomer both occur at M + 1. Hence, it was necessary to account for the contribution of naturally occurring isotopes to the signal of the ^{15}N isotopomer. This was achieved by calculating the natural (i.e. unlabelled) isotope distribution of each amino acid derivative using an online isotope distribution calculator (https://www.sisweb.com/mstools/isotope.htm) to account for natural abundance. The compound-specific method, which accurately quantifies 13 amino acids, captured about 50% of the total depolymerization rate determined by the bulk method described above.

2.7. Soil enzyme activities and microbial C and P use efficiency

We measured the potential activities of seven hydrolytic enzymes involved in SOM decomposition. β-1,4-glucosidase (BG), β-d-cellobiosidase (CB), α-glucosidase (AG), and β-xylosidase (Bxyl) are enzymes targeting C-rich substrates; β-1,4-*N*-acetylglucosaminidase (NAG) and leucine aminopeptidase (LAP) target N-rich substrates while Phosphatase (Pho) target P-rich substrates. Enzyme assays were conducted using standard fluorometric techniques described by Bell et al. (2013). Briefly, 2 g of frozen soil was blended with 60 mL of 50 mM sodium acetate buffer (pH = 5.2) for 1 minute. 800 µL of soil slurry was transferred on duplicate to a 96-deep-well microplate containing 200 µL of substrate solution. Duplicate quenched standards were made by adding 800 µl of soil slurry to 200 µL of either 4 methylumbelliferone (MUB), or 7-amino-4-methyl coumarin (MUC) at different concentration ranging from 0 µM to 100 µM for each soil. Soil slurries with fluorometric substrates were incubated for 3 h at 25°C. After the incubation period, plates were centrifuged for 2 min at 2000 x g after which 250 µL of soil slurry was transferred from the deep well plate into corresponding wells in black flat-bottomed 96-well plate and then scanned on a CLARIOstar plate reader (BMG LABTECH, Germany) using excitation at 365 nm and emission at 450 nm. Units for all enzyme nutrient acquisition activities are expressed as nmol activity g^{-1} dry soil h^{-1}.

Microbial carbon use efficiency (CUE) and phosphorus use efficiency (PUE) were calculated from enzyme activity rates (Sinsabaugh et al., 2016). This calculation uses the elemental stoichiometry of SOM and microbial biomass, and the ratios of C to N-acquiring ecoenzymatic activities (Equations 3 and 4) in order to capture microbial adjustments in resource use efficiency in response to substrate stoichiometry (Schimel et al., 2022).

$$CUE_{C:P} = CUE_{max}\left(\frac{S_{C:P}}{S_{C:P}+K}\right) \quad \text{where} \quad S_{C:N} = 1 \times \frac{B_{C:P}}{EEA_{C:P}} \tag{3}$$

$$PUE_{P:C} = PUE_{max}\left(\frac{S_{P:C}}{S_{P:C}+K}\right) \quad \text{where} \quad S_{P:C} = (1 - EEA_{P:C}) \times \frac{B_{P:C}}{L_{P:C}} \tag{4}$$

Where $S_{C:P}$ is a scalar that quantifies how ecoenzymatic activities allocate resources to mitigate differences between the elemental composition of available resources and that of microbial biomass. CUE_{max} is set at 0.6, PUE_{max} is set at 1.0 and K is the half saturation constant set at 0.5 (Sinsabaugh et al., 2016). $EEA_{C:P}$ refers to the enzymatic BG:Pho ratio, $B_{C:P}$ is the microbial C:P ratio and $L_{C:P}$ is the soil DOC:Bray-P ratio.

2.8. Statistical analyses

Statistical analyses were carried out with Rstudio software (version 4.1.0, R Core Team, 2021). Linear mixed effect models were used to evaluate eCO_2 effect (ambient/elevated), P addition (fertilised/unfertilised) effect, time effect and their interactions set as fixed effects, with ring set as random effect (“lmer” function, lme4 package; Bates et al., 2015). Significance was determined using

Type II ANOVA tests applied to the fitted mixed models and a Tukey's multi-comparison test was performed when eCO_2 or P addition had an effect. For each variable, two linear mixed models were produced. One with the effect of eCO_2 and time and their interactions as fixed factors over the three sampling times (March, April and May) sampled in the —P squares for April and May. And one with the additional effect of P addition (and its interactions) over two sampling times (April and May). Log transformations were performed when the assumptions of normality and variance were not met. IER data were analysed with similar mixed models, one comprising eCO_2 and time over the 16 months assessed and one with the P addition effect as an additional fixed effect over the two months of addition. Compound specific amino acid rates were analysed at one time step (April) in a model comprising eCO_2 effect, P addition and amino acids (13 AA). We acknowledge that the low number of replicate FACE rings (n = 2) limits statistical power, as is typical for large-scale FACE experiments. To improve reliability of the treatment effect, we used four subsampling locations within each plot, repetitive measurement over time, and applied mixed-effects models that account for variability between ring.

3. Results

3.1. Effect of eCO_2

3.1.1. Nutrients, microbial pools, root biomass and soil water

eCO_2 had a significant positive effect on soil nitrate concentration in the three months of soil sampling (+ 33%; Fig. 2A). Consistent with this increase, nitrate availability from IER measurements (Fig. 2D) showed a time dependent increase under eCO_2, from December 2021 to October 2022, and from March to May 2023, nitrate almost doubled under eCO_2. eCO_2 had a negative effect on MBC (—15%; $p = 0.01$, Table 1). Lower MBC led to lower microbial C:N and C:P ratios under eCO_2 ($p < 0.05$; Table 1; Fig. S2). Fine root biomass was 30% lower under eCO_2 ($p = 0.006$; Table 1; Fig. S2). Soil gravimetric moisture was consistently lower under eCO_2 (—14%; $p = 0.1$) and was negatively correlated with soil nitrate (Fig. S3). No eCO_2 effects were detected on ammonium, DOC nor on MBN and MBP pools (Fig. 2 and Table 1).

Table 1
ANOVA p-values for the effect of eCO_2 in the first model (eCO_2 alone; three time points), and of P-addition (Ferti) and eCO_2 and their interactions in the second model (Ferti x eCO_2; two time points). Significant effects ($p < 0.05$) are shown in bold.

Factors	*Pre and post addition: March-May*	*Post addition: April and May*		
	eCO_2	*Ferti*	*Ferti:eCO_2*	*Ferti:time*
DF	1	1	1	1
Gravimetric moisture	0.10	0.60	0.71	0.50
Fine root biomass	**0.006****	0.11	0.34	0.23
DOC	0.56	**0.008****	0.39	**0.006****
MBC	**0.04***	0.29	0.33	0.46
MBN	0.15	0.35	0.89	0.54
MBP	0.88	**0.0001*****	0.82	0.15
MBC:MBN	**0.02***	0.51	**0.03***	0.90
MBC:MBP	**0.004***	**0.0001*****	0.11	0.23
MBN:MBP	0.10	**< 0.0001****	0.86	0.20

3.1.2. Nitrogen fluxes and enzyme activities

eCO_2 had no effect on bulk N cycling rates (Fig. 3), compound specific depolymerization and immobilization (Fig. 4), microbial N use efficiency (NUE) nor on enzyme activities (Fig. 5). Gross mineralization and NH_4^+ immobilization showed a strong effect of time, with gross mineralization and NH_4^+ immobilization rates being five times higher in March compared to after fertilization (Fig. 3). Accordingly, microbial NUE showed an effect of time, as it was around 0.80 in March and increased to ~ 0.95 in April and May (Fig. 3).

3.2. Effect of P addition

3.2.1. Nutrient pools and ratios

P addition increased P pools while decreasing DOC and plant available N pools (NH_4^+, NO_3^-, FAA) in soil, independent from eCO_2 (Table 1). P addition increased soil Bray-P and MBP pools ($p < 0.05$; Fig. 2 and Table 1). While P was added as PO_4^{3-}, 60% of the additional P was found in MBP after 10 days and ~ 80% after 2 months (Fig. S4). MBC and MBN were not significantly increased by P addition leading to lower microbial biomass N:P and C:P ratios in fertilized plots (Fig. 2; $p < 0.05$). Microbial biomass C:N, however, showed an interactive effect of P addition x eCO_2, with lower C:N under eCO_2 in unfertilized plots and higher C:N in fertilized ones (Table 1; $p = 0.03$). Of the 13 free amino acids (FAAs), seven

showed lower concentrations following P addition (aspartic acid, glutamic acid, glycine, serine, threonine, tyrosine, and valine), driving the overall lower total AA concentration ($p < 0.01$; Fig. S5). While asparagine increased, particularly under eCO_2, and no changes were observed for the remaining amino acids (Fig. S5).

3.2.2. Nitrogen fluxes

P addition increased microbial N retention through opposing effects on N-mining (*i.e.*, mineralization and depolymerization) and on N immobilization (Fig. 3). Gross mineralization rates were 13% lower in the P-fertilized plots post P fertilization (April, May; $p = 0.04$) while NH_4^+ immobilization was 27% higher ($p = 0.11$; Fig. 3). Consequently, microbial NH_4^+ retention (NH_4^+ immobilization: gross mineralization ratio) was significantly higher in P-fertilized plots, in line with lower soil NH_4^+ (Fig. 2B).

After 10 days, P addition had no detectable effect on gross depolymerization or FAA immobilization, but FAA retention slightly increased ($p = 0.17$) following the same pattern as NH_4^+ retention. By May, two months post-addition, gross depolymerization and FAA immobilization decreased in P-fertilized plots under aCO_2 but were sustained under eCO_2. Consequently, depolymerization and FAA immobilization were 14% higher under eCO_2 in P-fertilized plots (Fig. 3). A similar pattern to bulk gross depolymerization in May was observed on compound specific depolymerization measured in April ($p = 0.006$; Fig. 4). Under P fertilisation, the eCO_2-induced increase in gross N depolymerization was primarily associated with higher production of alanine, glycine, proline, asparagine and aspartate, while increased amino acid immobilization involved alanine, glycine and proline together with glutamic acid and glutamate. Threonine decreased under both aCO_2 and eCO_2, while the other AA remained globally unaffected (valine, isoleucine, leucine, etc.; Fig. 4). Finally, NUE, calculated from bulk gross depolymerization and mineralization rates, remained unchanged as gross N mineralization followed the same pattern as depolymerization but with smaller magnitude and no statistically significant differences.

3.2.3. Enzyme activities

P addition had no immediate effect on enzyme activities after 10 days; however, it reduced all seven enzyme activities after two months compared to no P addition (Fig. S6). N-targeting enzymes were reduced more strongly under eCO_2 ($p = 0.08$; Fig. 5). However, C-targeting enzymes (BG, Bxyl, AG, CB) were reduced more strongly under aCO_2 than eCO_2 (– 79% under aCO_2 compared to – 44% under eCO_2) with P-targeting enzyme (Pho) showing a similar pattern (– 45% under aCO_2 compared to – 30% under eCO_2). Microbial PUE decreased under P addition ($p = 0.03$) while microbial CUE increased with P addition, particularly after two months ($p < 0.0001$; Fig. 5).

4. Discussion

4.1. P addition induced a shift in microbial strategy from resource acquisition to growth

P addition alone induced a reduction in SOM decomposition, as evidenced by the decrease in all seven enzyme activities and N cycling rates, noticeable two months after P addition. This suggests that microbial demand for P drives SOM decomposition under low P conditions (Rosinger et al., 2019) while indicating a strong coupling of C, N and P cycling in soils due to substrate stoichiometry (Manzoni et al., 2021; Spohn, 2015). However, microbes showed flexibility in their C:N:P stoichiometry as they stored about 80% of the added P without similar increase in microbial biomass C or N. This is consistent with the “luxury P uptake” strategy in P-limited soils where microbes retain P whenever available (Jiang et al., 2024a; Solovchenko et al., 2019). P addition also increased microbial CUE and N retention suggesting a more efficient recycling of C and N. Higher CUE suggests that before fertilization microbes were prioritizing enzyme production to acquire P, thereby diverting C away from growth and toward P-acquisition processes (X. Wang et al., 2022). Thus, in the short term, P addition redirected microbial activity from P acquisition toward growth, reducing SOM decomposition while increasing microbial retention of C, N and P.

4.2. eCO_2 enhances microbial C-N cycling once P limitation is alleviated

Following P addition, eCO_2 stimulated protein depolymerization as well as C- and P-targeting enzyme activities, indicating enhanced nutrient cycling under eCO_2 once P limitation was alleviated. Despite relatively low statical power due to FACE replication constraints, the consistency of responses across multiple independent measurements and convergent patterns in both bulk and compound-specific analyses increase confidence in the mechanistic interpretation of this acute response to P fertilization under eCO_2. At the compound specific level, the higher production and assimilation of alanine and glycine – central AA in microbial metabolism – suggests enhanced microbial C processing. Alanine is directly linked to C metabolism via its reversible conversion to pyruvate (Apostel et al., 2017), while glycine is involved in one-carbon (C1) metabolism, an anabolic process associated to high CUE (Bruinsma et al., 2023). Higher glycine assimilation was previously observed under eCO_2 and was supposed to favour microbial C routing (Andresen et al., 2014). In parallel, the increased assimilation of glutamic acid and glutamate confirms an intensified microbial anabolism as these AA are the main intracellular N donors for anabolic processes (Walker et al., 2016). Their enhanced assimilation could have promoted the synthesis of aspartic acid and subsequently asparagine, via transamination reactions (Apostel et al., 2013; Knowles et al., 2010), potentially explaining the higher production rates of these AA without concomitant assimilation. Taken together, the response of these specific AA reflects enhanced microbial biosynthesis (e.g., C1 metabolism; Fig. 6), suggesting that additional C supplied under eCO_2 is more efficiently used for microbial growth once P limitation was relieved. This is consistent with the observed increase in MBC under eCO_2 after P fertilization, reducing the initial apparent C limitation observed under eCO_2 (low MBC despite higher C available; Jiang et al., 2020). Hence, eCO_2 appears to

enhance AA turn-over and anabolic processes once P limitation is relieved. However, it is unclear if this will translate into higher available N for plants as AA appear to be efficiently immobilized and only asparagine showed an increased in concentration. Thus, our results highlight that P limitation in forest ecosystem hinders higher C cycling and soil C retention under eCO_2 by restricting the microbial capacity to process and retain additional C.

4.1. Shift towards N limitation?

Alleviating P limitation initiated a shift toward N limitation as observed by the reduction in soil available N pools by 30%, reflected by NO_3^-, NH_4^+ and FAA pools. This reduction in N availability due to a tightening of microbial N cycling is consistent with previous observations on P fertilization experiments (Mehnaz et al., 2019; R. Wang et al., 2022) and supports our second hypothesis. However, it remains unclear if this shift to N limitation was exacerbated under eCO_2. While N depolymerization and AA immobilization were faster under eCO_2, soil nitrate concentrations remained consistently higher under eCO_2 (~ + 30%) even after P fertilization. Higher nitrate under eCO_2 was previously observed at the same site after six months and after five years of CO_2 enrichment (Hasegawa et al., 2016; Pihlblad et al., 2023), as well as at canopy FACE in a Swiss mature forest (Schleppi et al., 2012). Nitrate accumulation under eCO_2 may be indicative of P limitation because of reduced nitrate plant uptake (Mrak et al., 2024), in contrast to N-limited systems where eCO_2 enhances plant N uptake and deplete soil nitrate (Kourmouli et al., 2025; Rumeau et al., 2024). Hence, that nitrate remained high under eCO_2 suggests that the system has not yet transitioned into a strongly N limited state; however, if enhanced microbial growth and N immobilization persist then N limitation could intensify over time. At the same time, evidence for plant-level P limitation following P addition is weak. Although microbial immobilization captured most of the added P, the remaining portion was nearly sufficient to meet the full annual plant P demand at the site (~ 0.4 g m^{-2}; (Jiang et al., 2024a), providing little evidence for P limitation. Hence, our findings suggest that P addition initiated a shift toward N limitation that is likely to intensify with time under eCO_2. In the short term, however, the ecosystem resides in a transient state between N and P limitation. During this transitional phase, eCO_2 promotes microbial C retention and potentially plant C storage because neither nutrients constraint photosynthesis and net primary productivity. Nevertheless, the longevity of this transient window remains to be resolved.

5. Conclusion

Using the unique, large-scale ecosystem P manipulation under long-term CO_2 enrichment of a mature *Eucalyptus* forest, and a high-resolution, multifaceted assessment of microbial processes, this study shows that relaxing P limitation shifted soil microbial strategies from P acquisition to microbial growth. As microbes invested less in P-mobilizing enzymes and more in biomass growth, they retained a greater proportion of available N, reducing soil N and pushing the system toward lower N availability, increasing the potential for plant-level N limitation. Under eCO_2, this shift towards microbial growth with P addition was even exacerbated, as evidenced by the targeted enhanced assimilation of AA involved in

biosynthesis pathways. Collectively, our results indicate that alleviating P limitation can rapidly stimulate C-N cycling under eCO_2, shifting microbial N demand and promoting microbial C retention in soils. However, over longer timescales, this may drive the ecosystem toward N limitation and limit the CO_2 fertilization effect. This would contrast expectations that P supplementation may be a viable strategy to enable CO_2 stimulation of productivity in these and other low P forests. More broadly, our findings highlight the central role of microbial C and nutrient metabolism in shaping ecosystem responses to future CO_2-enriched atmospheres.

Declarations

AUTHOR CONTRIBUTIONS

Dr. Manon Rumeau: conceptualization, investigation, methodology, visualization, writing original draft. Dr. Yolima Carillo: conceptualization, methodology, resources, writing – reviews. Dr. Fotis Sgouridis: resources, writing – reviews. Dr. Catriona MacDonald: resources, writing – reviews. Paola Pisetta Raupp: investigation, writing – reviews. Dr. Charles Warren: resources, writing – reviews. M.R., Y.C. and S.U. conceptualized the work. M.R. and P.P.R. performed formal analysis. Dr. Michaela K. Reay: writing – reviews. Prof. Rob MacKenzie: funding acquisition, writing – reviews. Prof. Sami Ullah: conceptualization, funding acquisition and writing – reviews.

ACKNOWLEDGMENTS

We would like to thank the Technical Team at Euc-FACE (Dr. Vinod Kumar and Craig McNamara), who maintains and operates the experimental FACE infrastructure making access for research to address questions of (inter)national significance. This work was funded by the UKRI NERC Large grants – Qinquennial (half-decadal) carbon and nutrient dynamics in temperate forests: Implications for carbon sequestration in a high carbon dioxide world (QUINTUS; NE/S015833/1).

References

1. Andresen, L.C., Carrillo, Y., Macdonald, C.A., Castañeda-Gómez, L., Bodé, S., Rütting, T., 2020. Nitrogen dynamics after two years of elevated CO2 in phosphorus limited Eucalyptus woodland. Biogeochemistry 150, 297–312. https://doi.org/10.1007/s10533-020-00699-y
2. Andresen, L.C., Dungait, J.A.J., Bol, R., Selsted, M.B., Ambus, P., Michelsen, A., 2014. Bacteria and Fungi Respond Differently to Multifactorial Climate Change in a Temperate Heathland, Traced with 13C-Glycine and FACE CO2. PLoS ONE 9, e85070. https://doi.org/10.1371/journal.pone.0085070
3. Apostel, C., Dippold, M., Glaser, B., Kuzyakov, Y., 2013. Biochemical pathways of amino acids in soil: Assessment by position-specific labeling and 13C-PLFA analysis. Soil Biol. Biochem. 67, 31–40. https://doi.org/10.1016/j.soilbio.2013.08.005

4. Apostel, C., Dippold, M.A., Bore, E., Kuzyakov, Y., 2017. Sorption of Alanine changes microbial metabolism in addition to availability. Geoderma 292, 128–134. https://doi.org/10.1016/j.geoderma.2017.01.016
5. Brookes, P.C., Landman, A., Pruden, G., Jenkinson, D.S., 1985. Chloroform fumigation and the release of soil nitrogen: A rapid direct extraction method to measure microbial biomass nitrogen in soil. Soil Biol. Biochem. 17, 837–842. https://doi.org/10.1016/0038-0717(85)90144-0
6. Bruinsma, L., Wenk, S., Claassens, N.J., Martins Dos Santos, V.A.P., 2023. Paving the way for synthetic C1 - Metabolism in Pseudomonas putida through the reductive glycine pathway. Metab. Eng. 76, 215–224. https://doi.org/10.1016/j.ymben.2023.02.004
7. Chen, Y., Sun, T.-T., Qian, H.-Y., Fan, J.-B., He, Y.-Q., Sun, B., 2016. Nitrogen mineralization as a result of phosphorus supplementation in long-term phosphate deficient soil. Appl. Soil Ecol. 106, 24–32. https://doi.org/10.1016/j.apsoil.2016.04.019
8. Cheng, Y., Wang, J., Sun, N., Xu, M., Zhang, J., Cai, Z., Wang, S., 2018. Phosphorus addition enhances gross microbial N cycling in phosphorus-poor soils: a 15N study from two long-term fertilization experiments. Biol. Fertil. Soils 54, 783–789. https://doi.org/10.1007/s00374-018-1294-5
9. Cleveland, C.C., Liptzin, D., 2007. C:N:P stoichiometry in soil: is there a “Redfield ratio” for the microbial biomass? Biogeochemistry 85, 235–252. https://doi.org/10.1007/s10533-007-9132-0
10. Crous, K.Y., Ósvaldsson, A., Ellsworth, D.S., 2015. Is phosphorus limiting in a mature Eucalyptus woodland? Phosphorus fertilisation stimulates stem growth. Plant Soil 391, 293–305. https://doi.org/10.1007/s11104-015-2426-4
11. Crous, K.Y., Wujeska-Klause, A., Jiang, M., Medlyn, B.E., Ellsworth, D.S., 2019. Nitrogen and Phosphorus Retranslocation of Leaves and Stemwood in a Mature Eucalyptus Forest Exposed to 5 Years of Elevated CO2. Front. Plant Sci. 10, 664. https://doi.org/10.3389/fpls.2019.00664
12. Cunha, H.F.V., Andersen, K.M., Lugli, L.F., Santana, F.D., Aleixo, I.F., Moraes, A.M., Garcia, S., Di Ponzio, R., Mendoza, E.O., Brum, B., Rosa, J.S., Cordeiro, A.L., Portela, B.T.T., Ribeiro, G., Coelho, S.D., De Souza, S.T., Silva, L.S., Antonieto, F., Pires, M., Salomão, A.C., Miron, A.C., De Assis, R.L., Domingues, T.F., Aragão, L.E.O.C., Meir, P., Camargo, J.L., Manzi, A.O., Nagy, L., Mercado, L.M., Hartley, I.P., Quesada, C.A., 2022. Direct evidence for phosphorus limitation on Amazon forest productivity. Nature 608, 558–562. https://doi.org/10.1038/s41586-022-05085-2
13. Darrouzet-Nardi, A., Ladd, M.P., Weintraub, M.N., 2013. Fluorescent microplate analysis of amino acids and other primary amines in soils. Soil Biol. Biochem. 57, 78–82. https://doi.org/10.1016/j.soilbio.2012.07.017
14. Davidson, E.A., Hart, S.C., Shanks, C.A., Firestone, M.K., 1991. Measuring gross nitrogen mineralization, and nitrification by 15 N isotopic pool dilution in intact soil cores. J. Soil Sci. 42, 335–349. https://doi.org/10.1111/j.1365-2389.1991.tb00413.x
15. Díaz, S., Grime, J.P., Harris, J., McPherson, E., 1993. Evidence of a feedback mechanism limiting plant response to elevated carbon dioxide. Nature 364, 616–617. https://doi.org/10.1038/364616a0

16. Du, E., Terrer, C., Pellegrini, A.F.A., Ahlström, A., Van Lissa, C.J., Zhao, X., Xia, N., Wu, X., Jackson, R.B., 2020. Global patterns of terrestrial nitrogen and phosphorus limitation. Nat. Geosci. 13, 221–226. https://doi.org/10.1038/s41561-019-0530-4
17. Ellsworth, D.S., Anderson, I.C., Crous, K.Y., Cooke, J., Drake, J.E., Gherlenda, A.N., Gimeno, T.E., Macdonald, C.A., Medlyn, B.E., Powell, J.R., Tjoelker, M.G., Reich, P.B., 2017. Elevated CO2 does not increase eucalypt forest productivity on a low-phosphorus soil. Nat. Clim. Change 7, 279–282. https://doi.org/10.1038/nclimate3235
18. Friedlingstein, P., Le Quéré, C., O'Sullivan, M., Hauck, J., Landschützer, P., Luijkx, I.T., Li, H., Van Der Woude, A., Schwingshackl, C., Pongratz, J., Regnier, P., Andrew, R.M., Bakker, D.C.E., Canadell, J.G., Ciais, P., Gasser, T., Jones, M.W., Lan, X., Morgan, E., Olsen, A., Peters, G.P., Peters, W., Sitch, S., Tian, H., 2025. Emerging climate impact on carbon sinks in a consolidated carbon budget. Nature. https://doi.org/10.1038/s41586-025-09802-5
19. Griffiths, B.S., Spilles, A., Bonkowski, M., 2012. C:N:P stoichiometry and nutrient limitation of the soil microbial biomass in a grazed grassland site under experimental P limitation or excess. Ecol. Process. 1, 6. https://doi.org/10.1186/2192-1709-1-6
20. Halbritter, 2020. The handbook for standardised field and laboratory measurements in terrestrial climate-change experiments and observational studies (ClimEx). Methods in Ecology and Evolution, 11 (1):22–37. URL https://climexhandbook.w.uib.no/2019/11/06/soil-microbial-biomass-c-n-and-p/ (accessed 7.15.24).
21. Hart, S.C., Nason, G.E., Myrold, D.D., Perry, D.A., 1994. Dynamics of Gross Nitrogen Transformations in an Old-Growth Forest: The Carbon Connection. Ecology 75, 880–891. https://doi.org/10.2307/1939413
22. Hasegawa, S., Macdonald, C.A., Power, S.A., 2016. Elevated carbon dioxide increases soil nitrogen and phosphorus availability in a phosphorus-limited *Eucalyptus* woodland. Glob. Change Biol. 22, 1628–1643. https://doi.org/10.1111/gcb.13147
23. Hasegawa, S., Piñeiro, J., Ochoa-Hueso, R., Haigh, A.M., Rymer, P.D., Barnett, K.L., Power, S.A., 2018. Elevated CO_2 concentrations reduce C_4 cover and decrease diversity of understorey plant community in a *Eucalyptus* woodland. J. Ecol. 106, 1483–1494. https://doi.org/10.1111/1365-2745.12943
24. Jakobsen, I., Smith, S.E., Smith, F.A., Watts-Williams, S.J., Clausen, S.S., Grønlund, M., 2016. Plant growth responses to elevated atmospheric CO_2 are increased by phosphorus sufficiency but not by arbuscular mycorrhizas. J. Exp. Bot. 67, 6173–6186. https://doi.org/10.1093/jxb/erw383
25. Jiang, M., Crous, K.Y., Carrillo, Y., Macdonald, C.A., Anderson, I.C., Boer, M.M., Farrell, M., Gherlenda, A.N., Castañeda-Gómez, L., Hasegawa, S., Jarosch, K., Milham, P.J., Ochoa-Hueso, R., Pathare, V., Pihlblad, J., Piñeiro, J., Powell, J.R., Power, S.A., Reich, P.B., Riegler, M., Zaehle, S., Smith, B., Medlyn, B.E., Ellsworth, D.S., 2024a. Microbial competition for phosphorus limits the CO2 response of a mature forest. Nature. https://doi.org/10.1038/s41586-024-07491-0

26. Jiang, M., Medlyn, B.E., Drake, J.E., Duursma, R.A., Anderson, I.C., Barton, C.V.M., Boer, M.M., Carrillo, Y., Castañeda-Gómez, L., Collins, L., Crous, K.Y., De Kauwe, M.G., Dos Santos, B.M., Emmerson, K.M., Facey, S.L., Gherlenda, A.N., Gimeno, T.E., Hasegawa, S., Johnson, S.N., Kännaste, A., Macdonald, C.A., Mahmud, K., Moore, B.D., Nazaries, L., Neilson, E.H.J., Nielsen, U.N., Niinemets, Ü., Noh, N.J., Ochoa-Hueso, R., Pathare, V.S., Pendall, E., Pihlblad, J., Piñeiro, J., Powell, J.R., Power, S.A., Reich, P.B., Renchon, A.A., Riegler, M., Rinnan, R., Rymer, P.D., Salomón, R.L., Singh, B.K., Smith, B., Tjoelker, M.G., Walker, J.K.M., Wujeska-Klause, A., Yang, J., Zaehle, S., Ellsworth, D.S., 2020. The fate of carbon in a mature forest under carbon dioxide enrichment. Nature 580, 227–231. https://doi.org/10.1038/s41586-020-2128-9

27. Jiang, M., Medlyn, B.E., Wårlind, D., Knauer, J., Fleischer, K., Goll, D.S., Olin, S., Yang, X., Yu, L., Zaehle, S., Zhang, H., Lv, H., Crous, K.Y., Carrillo, Y., Macdonald, C., Anderson, I., Boer, M.M., Farrell, M., Gherlenda, A., Castañeda-Gómez, L., Hasegawa, S., Jarosch, K., Milham, P., Ochoa-Hueso, R., Pathare, V., Pihlblad, J., Nevado, J.P., Powell, J., Power, S.A., Reich, P., Riegler, M., Ellsworth, D.S., Smith, B., 2024b. Carbon-phosphorus cycle models overestimate CO_2 enrichment response in a mature *Eucalyptus* forest. Sci. Adv. 10, eadl5822. https://doi.org/10.1126/sciadv.adl5822

28. Jones, D., 2002. Simple method to enable the high resolution determination of total free amino acids in soil solutions and soil extracts. Soil Biol. Biochem. 34, 1893–1902. https://doi.org/10.1016/S0038-0717(02)00203-1

29. Knowles, T.D.J., Chadwick, D.R., Bol, R., Evershed, R.P., 2010. Tracing the rate and extent of N and C flow from 13C,15N-glycine and glutamate into individual de novo synthesised soil amino acids. Org. Geochem. 41, 1259–1268. https://doi.org/10.1016/j.orggeochem.2010.09.003

30. Kourmouli, A., Hamilton, R.L., Pihlblad, J., Bartlett, R., MacKenzie, A.R., Hartley, I.P., Ullah, S., Shi, Z., 2025. Rapid Increase in Soil Respiration and Reduction in Soil Nitrate Availability Following CO2 Enrichment in a Mature Oak Forest. ACS Omega 10, 1624–1634. https://doi.org/10.1021/acsomega.4c09495

31. Manzoni, S., Chakrawal, A., Spohn, M., Lindahl, B.D., 2021. Modeling Microbial Adaptations to Nutrient Limitation During Litter Decomposition. Front. For. Glob. Change 4, 686945. https://doi.org/10.3389/ffgc.2021.686945

32. Mehnaz, K.R., Corneo, P.E., Keitel, C., Dijkstra, F.A., 2019. Carbon and phosphorus addition effects on microbial carbon use efficiency, soil organic matter priming, gross nitrogen mineralization and nitrous oxide emission from soil. Soil Biol. Biochem. 134, 175–186. https://doi.org/10.1016/j.soilbio.2019.04.003

33. Mooshammer, M., Wanek, W., Hämmerle, I., Fuchslueger, L., Hofhansl, F., Knoltsch, A., Schnecker, J., Takriti, M., Watzka, M., Wild, B., Keiblinger, K.M., Zechmeister-Boltenstern, S., Richter, A., 2014. Adjustment of microbial nitrogen use efficiency to carbon:nitrogen imbalances regulates soil nitrogen cycling. Nat. Commun. 5, 3694. https://doi.org/10.1038/ncomms4694

34. Mrak, K., Covre-Foltran, E., Lamersdorf, N., 2024. Elevated nitrate concentrations in soil solution under pure Douglas fir stands can be lowered by mixing with European beech and by site selection. For. Ecol. Manag. 564, 122004. https://doi.org/10.1016/j.foreco.2024.122004

35. Noll, L., Zhang, S., Zheng, Q., Hu, Y., Wanek, W., 2019. Wide-spread limitation of soil organic nitrogen transformations by substrate availability and not by extracellular enzyme content. Soil Biol. Biochem. 133, 37–49. https://doi.org/10.1016/j.soilbio.2019.02.016
36. Norby, R.J., 2025. Forest productivity response to elevated CO_2 in free-air CO_2 enrichment experiments: the 23 percent solution, revisited. New Phytol. 246, 1952–1959. https://doi.org/10.1111/nph.70162
37. Phillips, R.P., Finzi, A.C., Bernhardt, E.S., 2011. Enhanced root exudation induces microbial feedbacks to N cycling in a pine forest under long-term CO2 fumigation: Rhizosphere feedbacks in CO2-enriched forests. Ecol. Lett. 14, 187–194. https://doi.org/10.1111/j.1461-0248.2010.01570.x
38. Pihlblad, J., Andresen, L.C., Macdonald, C.A., Ellsworth, D.S., Carrillo, Y., 2023. The influence of elevated CO_2 and soil depth on rhizosphere activity and nutrient availability in a mature *Eucalyptus* woodland. Biogeosciences 20, 505–521. https://doi.org/10.5194/bg-20-505-2023
39. Piñeiro, J., Ochoa-Hueso, R., Serrano-Grijalva, L., Power, S.A., 2023. Phosphorus and water supply independently control productivity and soil enzyme activity responses to elevated CO2 in an understorey community from a Eucalyptus woodland. Plant Soil 483, 643–657. https://doi.org/10.1007/s11104-022-05763-0
40. Reich, P.B., Hobbie, S.E., Lee, T., Ellsworth, D.S., West, J.B., Tilman, D., Knops, J.M.H., Naeem, S., Trost, J., 2006. Nitrogen limitation constrains sustainability of ecosystem response to CO2. Nature 440, 922–925. https://doi.org/10.1038/nature04486
41. Rosinger, C., Rousk, J., Sandén, H., 2019. Can enzymatic stoichiometry be used to determine growth-limiting nutrients for microorganisms? - A critical assessment in two subtropical soils. Soil Biol. Biochem. 128, 115–126. https://doi.org/10.1016/j.soilbio.2018.10.011
42. Ross, G.M., Horn, S., Macdonald, C.A., Powell, J.R., Reynolds, J.K., Ryan, M.M., Cook, J.M., Nielsen, U.N., 2020. Metabarcoding mites: Three years of elevated CO2 has no effect on oribatid assemblages in a Eucalyptus woodland. Pedobiologia 81–82, 150667. https://doi.org/10.1016/j.pedobi.2020.150667
43. Rumeau, M., Sgouridis, F., MacKenzie, R., Carrillo, Y., Reay, M.K., Hartley, I.P., Ullah, S., 2024. The role of rhizosphere in enhancing N availability in a mature temperate forest under elevated CO2. Soil Biol. Biochem. 197, 109537. https://doi.org/10.1016/j.soilbio.2024.109537
44. Schimel, Bennett, J., 2004. Nitrogen mineralization: challenges of a changing paradigm. Ecology 85, 591–602. https://doi.org/10.1890/03-8002
45. Schimel, J., Weintraub, M.N., Moorhead, D., 2022. Estimating microbial carbon use efficiency in soil: Isotope-based and enzyme-based methods measure fundamentally different aspects of microbial resource use. Soil Biol. Biochem. 169, 108677. https://doi.org/10.1016/j.soilbio.2022.108677
46. Schleppi, P., Bucher-Wallin, I., Hagedorn, F., Körner, C., 2012. Increased nitrate availability in the soil of a mixed mature temperate forest subjected to elevated CO2 concentration (canopy FACE). Glob. Change Biol. 18, 757–768. https://doi.org/10.1111/j.1365-2486.2011.02559.x

47. Sinsabaugh, R.L., Turner, B.L., Talbot, J.M., Waring, B.G., Powers, J.S., Kuske, C.R., Moorhead, D.L., Follstad Shah, J.J., 2016. Stoichiometry of microbial carbon use efficiency in soils. Ecol. Monogr. 86, 172–189. https://doi.org/10.1890/15-2110.1
48. Solovchenko, A.E., Ismagulova, T.T., Lukyanov, A.A., Vasilieva, S.G., Konyukhov, I.V., Pogosyan, S.I., Lobakova, E.S., Gorelova, O.A., 2019. Luxury phosphorus uptake in microalgae. J. Appl. Phycol. 31, 2755–2770. https://doi.org/10.1007/s10811-019-01831-8
49. Spohn, M., 2015. Microbial respiration per unit microbial biomass depends on litter layer carbon-to-nitrogen ratio. Biogeosciences 12, 817–823. https://doi.org/10.5194/bg-12-817-2015
50. Terrer, C., Vicca, S., Hungate, B.A., Phillips, R.P., Prentice, I.C., 2016. Mycorrhizal association as a primary control of the CO_2 fertilization effect. Science 353, 72–74. https://doi.org/10.1126/science.aaf4610
51. Terrer, C., Vicca, S., Stocker, B.D., Hungate, B.A., Phillips, R.P., Reich, P.B., Finzi, A.C., Prentice, I.C., 2018. Ecosystem responses to elevated CO_2 governed by plant–soil interactions and the cost of nitrogen acquisition. New Phytol. 217, 507–522. https://doi.org/10.1111/nph.14872
52. Walker, M.C., Van Der Donk, W.A., 2016. The many roles of glutamate in metabolism. J. Ind. Microbiol. Biotechnol. 43, 419–430. https://doi.org/10.1007/s10295-015-1665-y
53. Wanek, W., Mooshammer, M., Blöchl, A., Hanreich, A., Richter, A., 2010. Determination of gross rates of amino acid production and immobilization in decomposing leaf litter by a novel 15N isotope pool dilution technique. Soil Biol. Biochem. 42, 1293–1302. https://doi.org/10.1016/j.soilbio.2010.04.001
54. Wang, R., Bicharanloo, B., Hou, E., Jiang, Y., Dijkstra, F.A., 2022. Phosphorus Supply Increases Nitrogen Transformation Rates and Retention in Soil: A Global Meta-Analysis. Earths Future 10, e2021EF002479. https://doi.org/10.1029/2021EF002479
55. Wang, X., Cui, Y., Wang, Y., Duan, C., Niu, Y., Sun, R., Shen, Y., Guo, X., Fang, L., 2022. Ecoenzymatic stoichiometry reveals phosphorus addition alleviates microbial nutrient limitation and promotes soil carbon sequestration in agricultural ecosystems. J. Soils Sediments 22, 536–546. https://doi.org/10.1007/s11368-021-03094-8
56. Wang, Y.P., Law, R.M., Pak, B., 2010. A global model of carbon, nitrogen and phosphorus cycles for the terrestrial biosphere. Biogeosciences 7, 2261–2282. https://doi.org/10.5194/bg-7-2261-2010
57. Warren, C.R., 2019. Isotope pool dilution reveals rapid turnover of small quaternary ammonium compounds. Soil Biol. Biochem. 131, 90–99. https://doi.org/10.1016/j.soilbio.2019.01.004
58. Wu, J., He, Z.-L., Wei, W.-X., O'Donnell, A.G., Syers, J.K., 2000. Quantifying microbial biomass phosphorus in acid soils. Biol. Fertil. Soils 32, 500–507. https://doi.org/10.1007/s003740000284
59. Zhu, Z., Piao, S., Myneni, R.B., Huang, M., Zeng, Z., Canadell, J.G., Ciais, P., Sitch, S., Friedlingstein, P., Arneth, A., Cao, C., Cheng, L., Kato, E., Koven, C., Li, Y., Lian, X., Liu, Y., Liu, R., Mao, J., Pan, Y., Peng, S., Peñuelas, J., Poulter, B., Pugh, T.A.M., Stocker, B.D., Viovy, N., Wang, X., Wang, Y., Xiao, Z., Yang, H., Zaehle, S., Zeng, N., 2016. Greening of the Earth and its drivers. Nat. Clim. Change 6, 791–795. https://doi.org/10.1038/nclimate3004

Figures

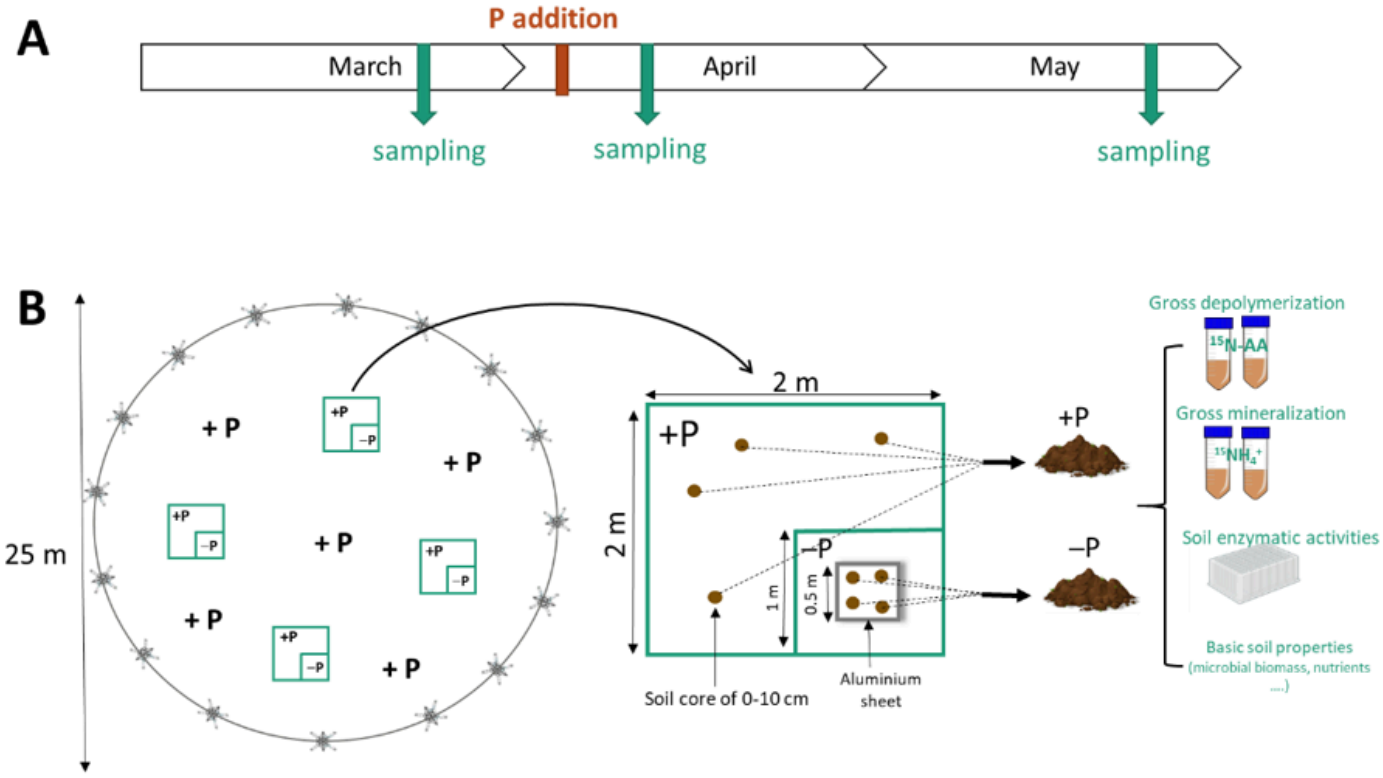


Figure 1

Schematic of A) P addition and sampling time across the three months of the experiment B) the sampling and processing for one FACE ring. Study plots in each ring were split into a fertilized area (+P) and an unfertilized, aluminium-enclosed area (—P). A series of microbial analyses were performed on the resulting soil samples.

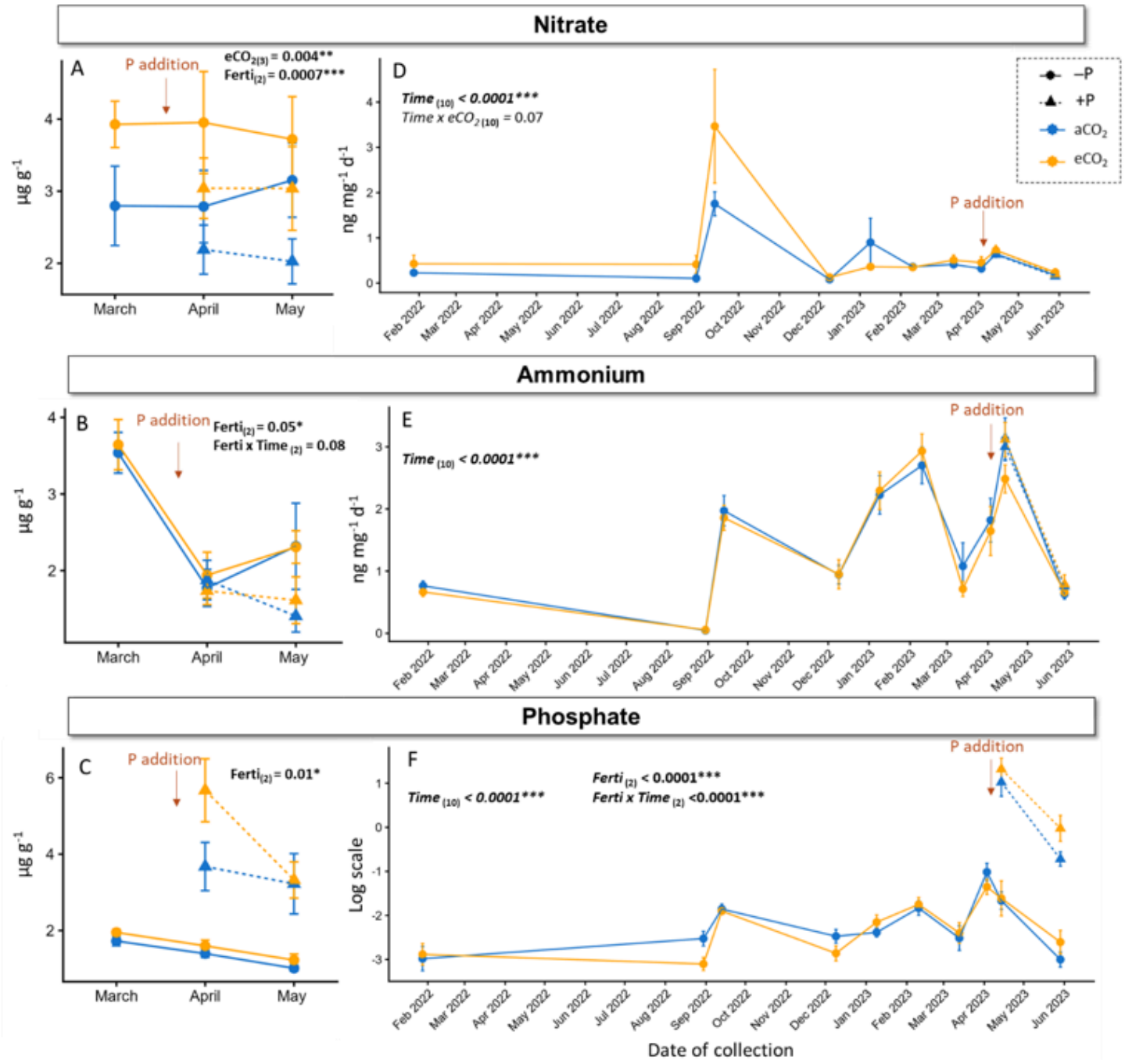


Figure 2

A) Nitrate, B) ammonium and C) Bray-P concentrations measured in soil sampled from March to May 2023. D) Nitrate, E) ammonium and F) phosphate availabilities measured by ion exchange resins (IER) from December 2021 to June 2023 in the six rings under eCO_2 (orange) and aCO_2 (blue) in both unfertilized (–P) and fertilized (+P) areas. When significant, ANOVA p-values are detailed for the effect of eCO_2, time and P-addition (Ferti) and their interactions. Number in subscript indicate the number of time points considered in the ANOVA. Data are means + SE (n=12).

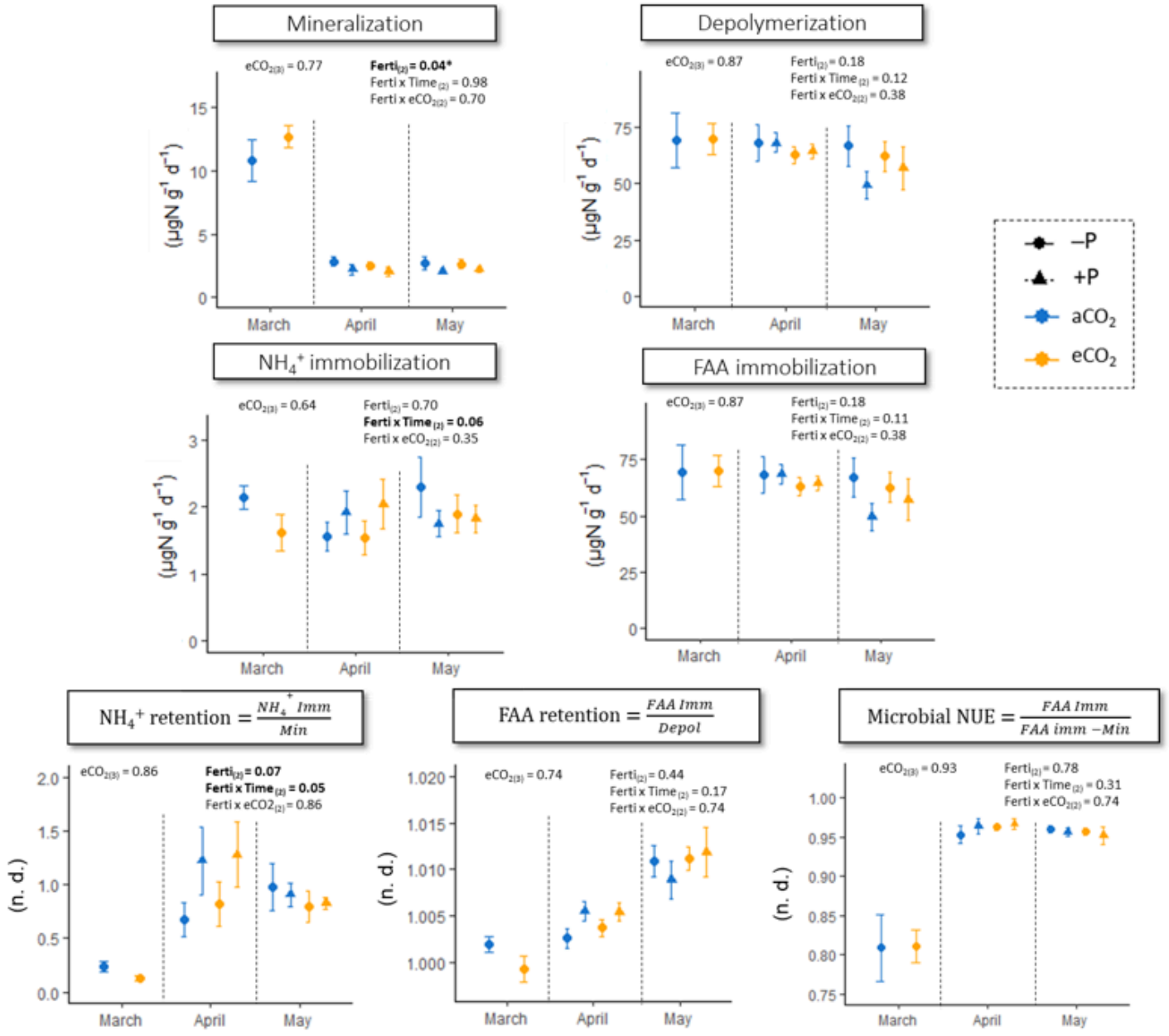


Figure 3

Ammonium and amino acids production, immobilization, microbial retention and microbial N use efficiency (NUE) in P-fertilized (+P) and non-P-fertilized (–P) plots under aCO_2 (blue) and eCO_2 (yellow) in March, April and May. Data are means + SE (n=8). Min = Mineralization, Imm= Immobilization, Depol = Depolymerization and n.d. = non dimensional.

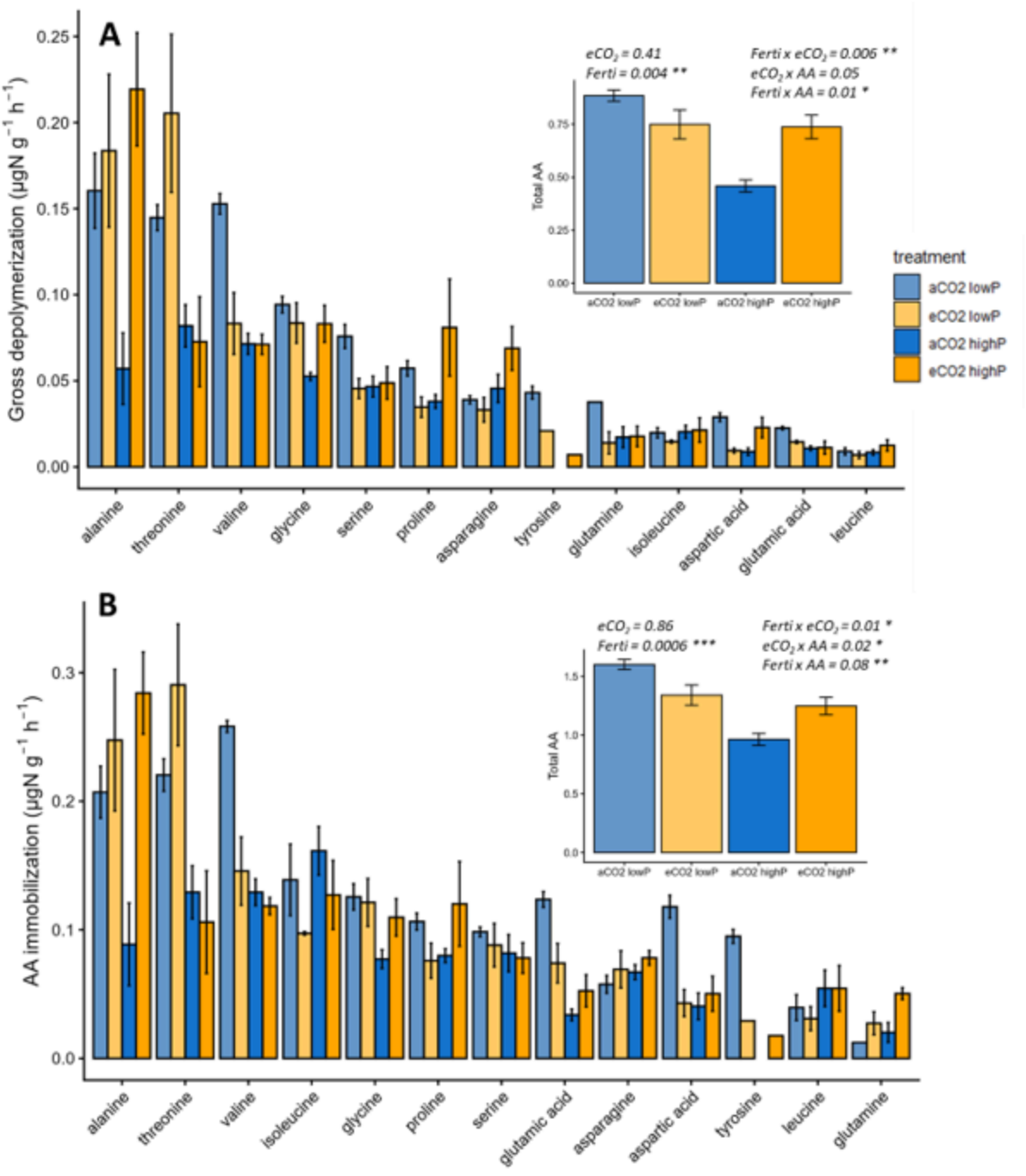


Figure 4

A) Compound specific depolymerization and B) AA immobilization rates in April for the 13 amino acids. Data are means + SE (n=4). The total rates are shown in the upper right of each plot. ANOVAs results are indicated for the total rates with eCO_2, Ferti and AA as fixed factors.

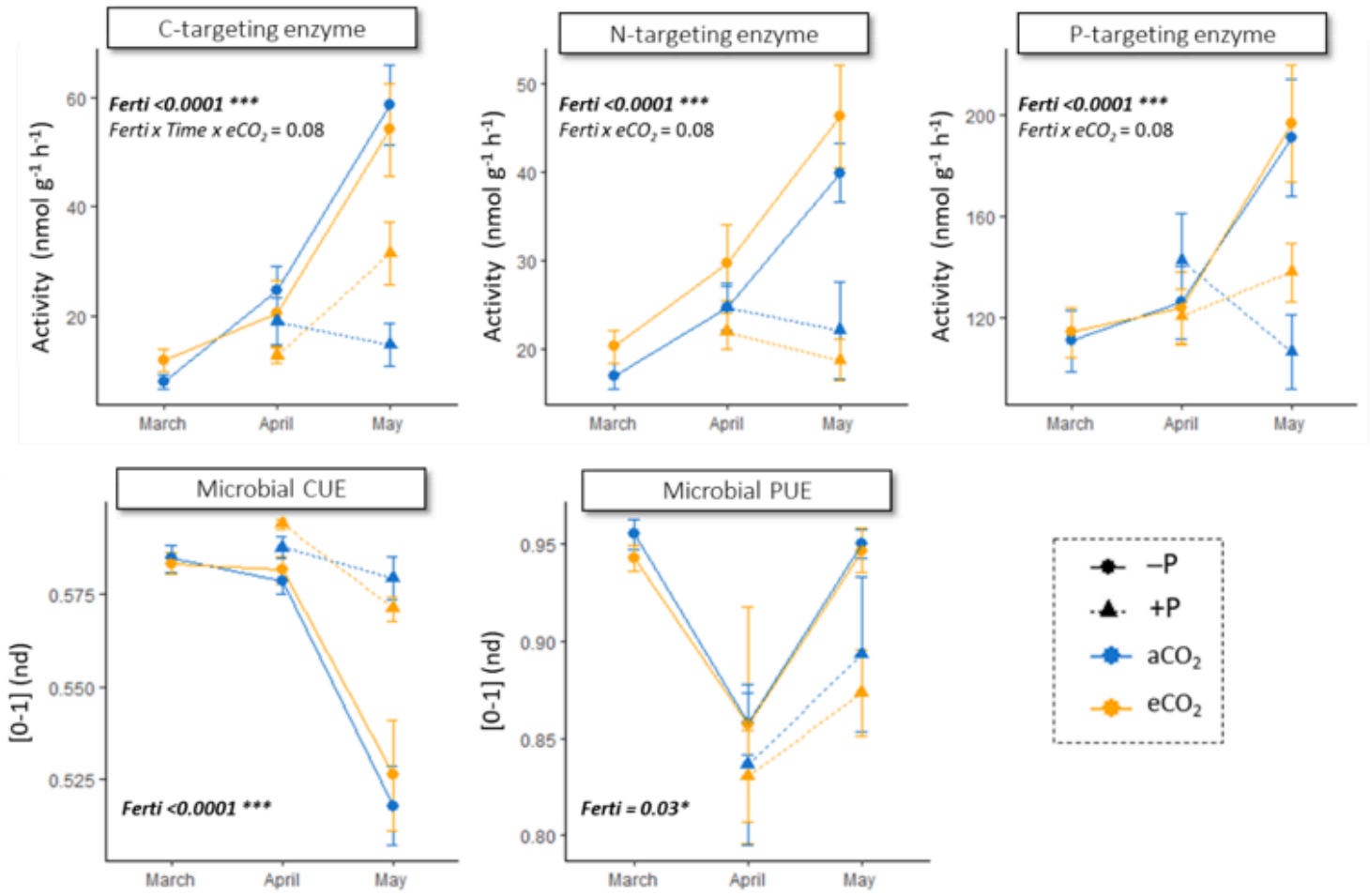


Figure 5

Soil enzymatic activities associated with C (BG, AG, CB, Bxyl), N (NAG, LAP) and P (Pho) cycling before (April) and after P-addition (April and May) in P-fertilized (+P) and non-P-fertilized (–P) plots under aCO_2 and eCO_2. Data are means + SE (n=8).

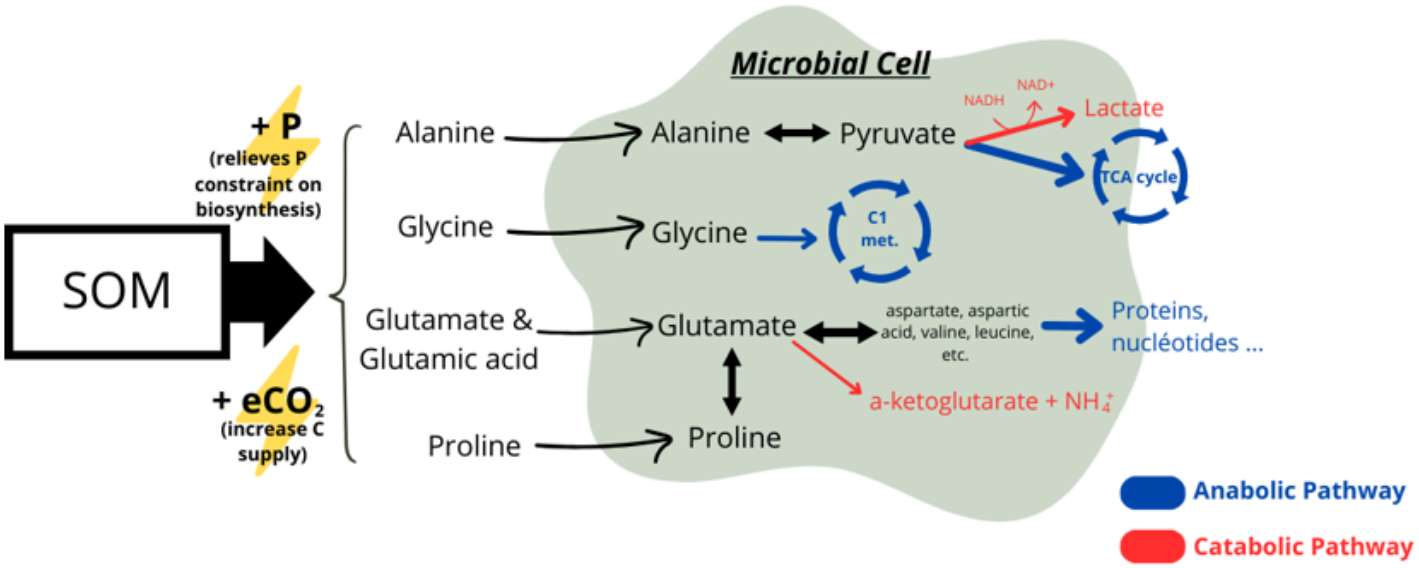


Figure 6

Conceptual model showing how phosphorus addition under elevated CO_2 influences amino acid (AA) depolymerization from soil organic matter (SOM) and intracellular processing in microbial cells. C1 met. = C1 metabolism; TCA cycle = tricarboxylic acid cycle.

Supplementary Files

This is a list of supplementary files associated with this preprint. Click to download.

- Graphicalabstract.png